Biochemical and Biophysical Research Communications 424 (2012) 348–353

Contents lists available at SciVerse ScienceDirect

Biochemical and Biophysical Research Communications

journal homepage: www.elsevier.com/locate/ybbrc

In vitro bio-functionality of gallium nitride sensors for radiation biophysics

Markus Hofstetter [a], John Howgate [b], Martin Schmid [a], Sebastian Schoell [b], Matthias Sachsenhauser [b], Denis Adigüzel [a], Martin Stutzmann [b], Ian D. Sharp [b,1], Stefan Thalhammer [a,*]

[a] Helmholtz Zentrum München, German Research Center for Environmental Health, Ingolstädter Landstrasse 1, D-85764 Neuherberg, Germany
[b] Walter Schottky Institut, Technische Universität München, Am Coulombwall 3, D-85748 Garching, Germany

ARTICLE INFO

Article history:
Received 19 June 2012
Available online 3 July 2012

Keywords:
Gallium nitride
Biocompatibility
Biofunctionality
Biomaterial
DNA double strand breaks
Ionizing radiation

ABSTRACT

There is an increasing interest in the integration of hybrid bio-semiconductor systems for the non-invasive evaluation of physiological parameters. High quality gallium nitride and its alloys show promising characteristics to monitor cellular parameters. Nevertheless, such applications not only request appropriate sensing capabilities but also the biocompatibility and especially the biofunctionality of materials. Here we show extensive biocompatibility studies of gallium nitride and, for the first time, a biofunctionality assay using ionizing radiation. Analytical sensor devices are used in medical settings, as well as for cell- and tissue engineering. Within these fields, semiconductor devices have increasingly been applied for online biosensing on a cellular and tissue level. Integration of advanced materials such as gallium nitride into these systems has the potential to increase the range of applicability for a multitude of test devices and greatly enhance sensitivity and functionality. However, for such applications it is necessary to optimize cell–surface interactions and to verify the biocompatibility of the semiconductor. In this work, we present studies of mouse fibroblast cell activity grown on gallium nitride surfaces after applying external noxa. Cell-semiconductor hybrids were irradiated with X-rays at air kerma doses up to 250 mGy and the DNA repair dynamics, cell proliferation, and cell growth dynamics of adherent cells were compared to control samples. The impact of ionizing radiation on DNA, along with the associated cellular repair mechanisms, is well characterized and serves as a reference tool for evaluation of substrate effects. The results indicate that gallium nitride does not require specific surface treatments to ensure biocompatibility and suggest that cell signaling is not affected by micro-environmental alterations arising from gallium nitride–cell interactions. The observation that gallium nitride provides no bio-functional influence on the cellular environment confirms that this material is well suited for future biosensing applications without the need for additional chemical surface modification.

1. Introduction

The coupling of semiconductor devices and biological material has drawn increasing interest for the analysis of intra- and extracellular signal fluxes [1,2]. While different kinds of sensors permit a variety of physical and chemical parameters to be recorded online, still the biocompatibility of the sensor materials has to be determined. It is generally assumed that the more biocompatible the surface is, the higher will be the degree of cell adhesion [3]. However, rigorous studies of biocompatibility extend beyond measures of the chemical inertness of the material–cell interface. Consequently, biocompatibility has been defined to apply to materials that minimally perturb the *in vivo* environment and that are likewise not adversely affected by the *in vivo* environment [4]. Nevertheless, information about biocompatibility and cytotoxicity of semiconductor materials is often deficient. Thus, negative effects on the host caused by material–cell interactions are frequently neglected when semiconductor devices are used as test systems on a cellular level.

In addition to microelectrode arrays [5–7], field effect transistors (FETs) [8] have also been implemented for *in vitro* recording of physiological signals. As shown in previous publications, AlGaN/GaN high electron mobility transistors have entered a wide variety of sensing applications [9–13]. Adding a thin capping layer, which covers the chemically less stable AlGaN layer results in GaN/AlGaN/GaN heterostructures. These devices can be rendered highly chemically inert and, thus, suitable for operation as solution-gated devices which are sensitive to surface potential- and pH-changes [10]. Furthermore, it has been determined that these devices are non-toxic to cells [11,15]. These characteristics have enabled the successful use of GaN-based heterostructures for biosensing applications [11–14].

* Corresponding author. Fax: +49 89 3187 3323.
E-mail address: stefan.thalhammer@helmholtz-muenchen.de (S. Thalhammer).
[1] Present address: Joint Center for Artificial Photosynthesis, Lawrence Berkeley National Laboratory, 1 Cyclotron Road, Berkeley, CA 94720, USA.

0006-291X/$ - see front matter © 2012 Elsevier Inc. All rights reserved.
http://dx.doi.org/10.1016/j.bbrc.2012.06.142

In order to apply sensors for the *in vitro* and *in vivo* detection of alterations in cell signaling processes, it is not only necessary to test and ensure the biocompatibility of the semiconductor substrates, but also to investigate the long-term biofunctionality of these surfaces. To this end, we have performed investigations of cell proliferation and growth dynamics on various differently treated gallium nitride surfaces. Compared to morphological investigations or analysis of cell-survival curves, measurements of changes in the cell repair mechanism provide advanced indicators for disturbed cell homeostasis. Here, DNA repair dynamics served as a retrospective detection tool to detect cellular alterations after applying ionizing radiation to cells cultivated on GaN surfaces. Since DNA suffers damage from free radicals and reactive oxygen species generated by ionizing radiation [16], the cell signaling was stimulated by X-rays. Organisms must trigger a series of events to promote repair of X-ray induced DNA damage in order to survive and restore chromosomal integrity [17]. Therefore, it is possible to investigate the alterations of these events arising from material-cell interactions by recording DNA repair dynamics of cells which are in direct contact with an extrinsic surface. By comparing cell repair mechanisms after the impact of external noxa on biocompatible reference materials, it is possible to exclude unwanted interactions with the substrate material and determine effects that are not detectable with morphological evaluation methods. DNA repair mechanisms occurring after radiation damage are well characterized [18] and are therefore suitable for investigations of bio-functionality.

2. Materials and methods

2.1. Material

Thin layers of the semiconductor material gallium nitride (GaN) were grown by a commercial metal-organic chemical vapor deposition (MOCVD) process on 330 μm thick c-plane sapphire substrates. Both n-type (silicon doped $n \approx 10^{18}\,\mathrm{cm}^{-3}$) and semi-insulating, iron compensated (6 MΩ at 300 K) films of 3.5 μm thickness were purchased from Lumilog (Vallauris, France). In addition, high electron mobility transistor (HEMT) structures, composed of a 2.9 μm carbon compensated GaN/72 nm nominally undoped GaN/25 nm $Al_{0.25}Ga_{0.75}N$/3 nm nominally undoped GaN cap layers were purchased from TopGaN (Warsaw, Poland). On top of a thin film stack of 1.5 μm undoped GaN/1.5 μm silicon-doped GaN, films of 0.5 μm magnesium doped GaN and 10 nm of adjusted magnesium doped GaN to $p \approx 10^{18}\,\mathrm{cm}^{-3}$ was purchased from TopGaN (Warsaw, Poland). These samples remained n-type due to the poor doping efficiency of Mg in GaN, but show reduced electron concentrations.

2.2. Surface functionalization

Both the glass and the GaN samples were cleaned with 70% ethanol and exposed to UV illumination for 20 min prior to functionalization and cell seeding. For sample preparation with a fibronectin layer, 1.25% of fibronectin stock solution (0.1% solution from bovine plasma, Sigma–Aldrich Biochemie, Germany) solved in HBSS (GIBCO Hank's balanced salt solution 1×, Invitrogen GmbH) was incubated on the sample surfaces at 37 °C for 20 min and after removing the supernatant air dried for 20 min under sterile conditions. Aminopropylsilane (APS) self-assembled monolayers were formed on GaN and glass surfaces from aminopropyldiethoxymethylsilane (APDMES) in a toluene solution in accordance with protocols published elsewhere [19,20]. Samples were stored in a light-shielded vacuum chamber and used for the experiments within 24 h after functionalization. Monolayer quality was assessed prior to use by static water contact angle measurements. The functionalization altered the contact angle from 80.1 ± 3.3° for an untreated GaN surface to 58.4 ± 4.2° for an APDEMS coated surface.

2.3. Cell culture

L929 mouse fibroblasts were cultured in RPMI media supplemented with 10% fetal calf serum and 1% antibiotic–antimycotic solution. Cells were incubated at 37 °C in 5% CO_2 atmosphere and 95% humidity and grown to a confluent layer. Before seeding them on the uncoated or functionalized sensor or glass surfaces, the cell cultures were trypsinized, centrifuged at 1000 rpm for 3 min and resuspended with new tissue medium to overcome trypsinization effects.

2.4. Immunostaining

Immunostaining was performed using anti-53BP1 (dianova, Hamburg, Germany), Alexa Fluor 488 (Invitrogen, Paisley PA4 9RF, UK), and Hoechst 33342 (Invitrogen, Paisley PA4 9RF, UK). After the irradiation procedure and repair times (30 min–24 h), cells were washed with PBS three times and fixed for immunofluorescent staining by incubation in glutaraldehyde (2% in PBS) or formaldehyde (2% in PBS) for 15 min, followed by permeabilization with Triton-X (0.15% in PBS) for 15 min at room temperature. Blocking was performed by incubation with BSA (0.1% in PBS) for 30 min. Immunostaining was accomplished with primary antibody 53BP1 (1:100 dilution in PBS) for 1 h at room temperature in a moist chamber, followed by a washing step with PBS (5 min), 0.15% Triton-X (10 min), PBS (5 min), and 0.2% BSA (7 min). Secondary antibody Alexa Fluor 488 (1:200 dilution in PBS) was incubated 1 h at room temperature in the dark. After a final washing step with PBS, cell nuclei were counterstained with Hoechst (1:500 solution in Hank's Balanced Salt Solution, HBSS) for 10 min and mounted in anti-fade solution Vectashield H-1000 (Vector Laboratories, Inc., Burlingame, CA).

2.5. Sample irradiation

To induce DNA double strand breaks, the cell cultures were irradiated with a medical X-ray system (Stabilipan TR300f, Siemens AG) equipped with a 4 mm Al filter. Reference measurements of the air kerma at the sample position were recorded with a dose area product meter (Diamentor M4, PTW, Germany). Cells grown on both gallium nitride and glass slides were exposed to low LET X-ray irradiation in an energy range from 50 to 150 keV. After specified waiting intervals following the exposure, the cells were fixed with glutaraldehyde or formaldehyde for immunofluorescence.

2.6. Image acquisition

All optical micrographs were acquired with a Zeiss Observer.Z1 equipped with a digital CCD camera (Rolera-XR, QImaging, Surrey, Canada). Transmitted light images were recorded using gallium nitride samples with polished sapphire back surfaces. For the investigation of DNA repair dynamics, foci were recorded with an LSM 510 laser scanning microscope (Zeiss, Germany). The foci were counted from Z-stacks recorded in 40 picture slices through the entire cell layer, with a distance of 0.3 μm between slices. For every sample at least 100 cells were evaluated.

2.7. AFM analysis

AFM investigations were performed with the NanoWizard I (JPK Instruments, Berlin, Germany) controlled by the JPK SPM Desktop

software (JPK Instruments, Berlin, Germany). Measurements of the surfaces were carried out at room temperature and ambient conditions using NSC15/AlBS cantilevers (MikroMasch, Estonia) with spring constants of 46 N/m and resonant frequencies of 325 kHz in tapping mode.

3. Results and discussion

3.1. Cell growth dynamics on gallium nitride

In order to investigate the bio-functionality of GaN surfaces it is essential to verify the degree of biocompatibility of the material. Therefore, fibronectin-coated GaN surfaces which are well characterized to provide excellent cell growth [12] were compared to oxygen terminated GaN surfaces, as well as amino-terminated molecular layers, covalently bound to GaN. Cell adhesion and morphology was investigated by optical transmission microscopy. Our experiments revealed that confluent layers on our samples typically formed within one day. To gain the highest contrast for comparison, we therefore show the results from within the first 24 h.

Cell growth studies were performed on GaN surfaces with comparable surface terminations. The final concentrations of L-929 fibroblasts were between 250 and 550 cells/mm^2 on all surfaces. Optical micrographs were obtained at intervals of 4 h, 6 h, and 24 h following cell seeding (Fig. 1). Cell proliferation and growth dynamics were compared on n-type Si-doped substrates and n-type Mg-compensated substrates. For both types of GaN substrates, oxygen terminated, fibronectin coated, and APS functionalized [21] surfaces were evaluated. As shown in Fig. 1, the cells started to adhere to the surface and exhibit their typical spindle like outer shape within the first 4 h. In fact, on fibronectin coated GaN surfaces, cell adhesion was observable only 1 h after cell seeding (data not shown). After 6 h of cell growth, visible variations in cell morphology can still be observed. However, after 24 h, we found a well-defined confluent monolayer of cells observable on all surfaces. The APS-functionalized GaN, providing a fully synthetic, non-buffering, and biocompatible sensor coating, showed no significant degradation nor an enhancement compared to untreated surfaces. The cells exhibited their typical spindle-like shape after 4 h. This indicates that APS-cell interactions are dominated by surface morphology, and biochemical effects play only a minor role compared to fibronectin coatings, which have a thickness of a several nm [22]. This conclusion is supported by the finding that only minor surface roughness changes are caused by the organosilane molecules, as determined by AFM measurements on the modified GaN surfaces (data not shown). Nevertheless, silanized surfaces can be advantageous for specific sensing applications, in which the layer provides the possibility for attachment of complex biomolecules such as DNA [23] or proteins [19,24,25] to the surface. A series of 10 consecutive experiments proved a very good reproducibility for all samples without any noticeable variations in either cell proliferation or growth dynamics. Therefore, while it is possible to enhance the early stage biocompatibility of the surfaces with proteins such as fibronectin, there are only slight variations in cell adherence after a cell growth time of 24 h.

Glassware such as crystallization beakers and optical glass slides is often used for cell seeding and is widely considered to be biocompatible. For this reason, we attempted a comparison between GaN and glass systems. Since both substrates are considered to be chemically inert and share similarly oxygen terminated surfaces, the cell proliferation and growth dynamics are expected to be in broad terms similar to one another if the surface roughness values are also comparable. Although AFM measurements show that the rms surface roughness of both n-type GaN and high quality glassware is approximately 1 nm in a 10 × 10 μm^2 area, the surface topography is significantly different (Fig. 2). The topography

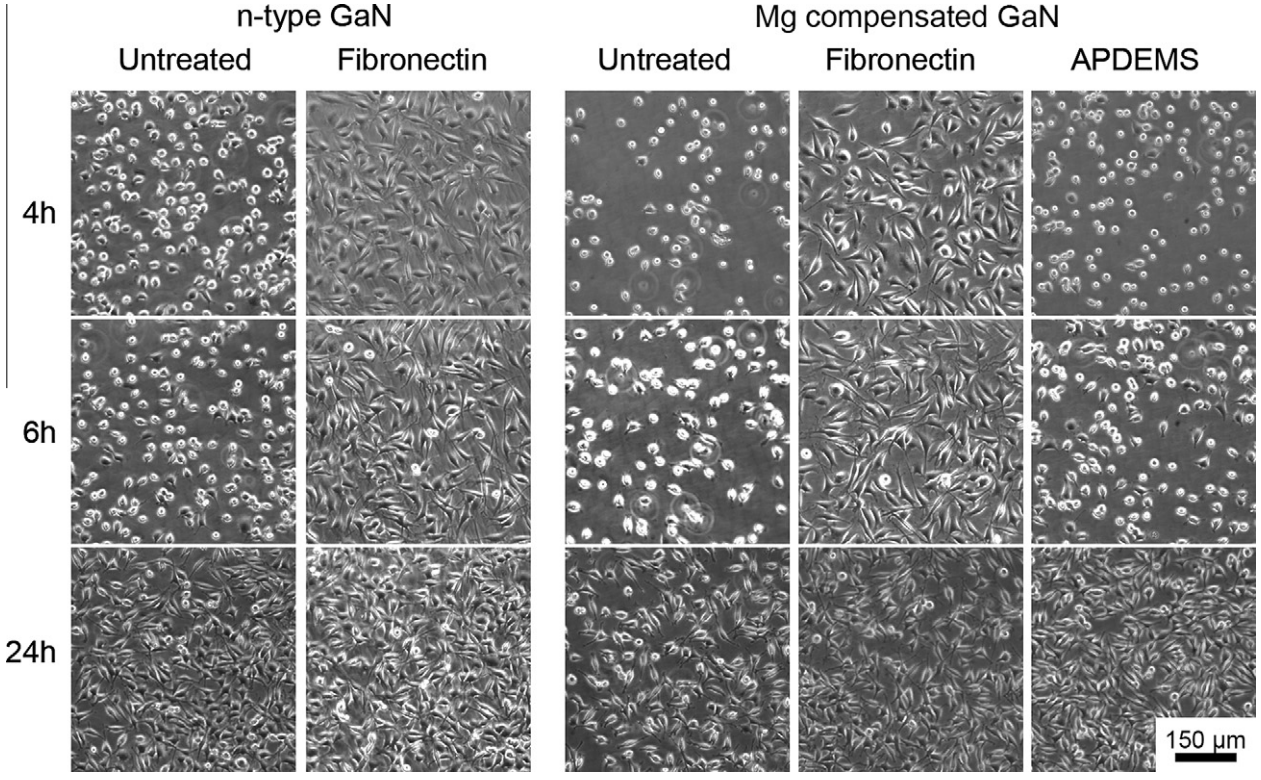

Fig. 1. Optical micrographs reveal the differences between untreated, fibronectin coated, and APS functionalized GaN surfaces at 4 h, 6 h and 24 h after cell seeding on the surfaces. After only 1 h, the cells showed the typical spindle-like shape on fibronectin coated GaN. Although there were visible variations in cell morphology after 6 h, a nearly confluent monolayer was achieved within 24 h for all samples.

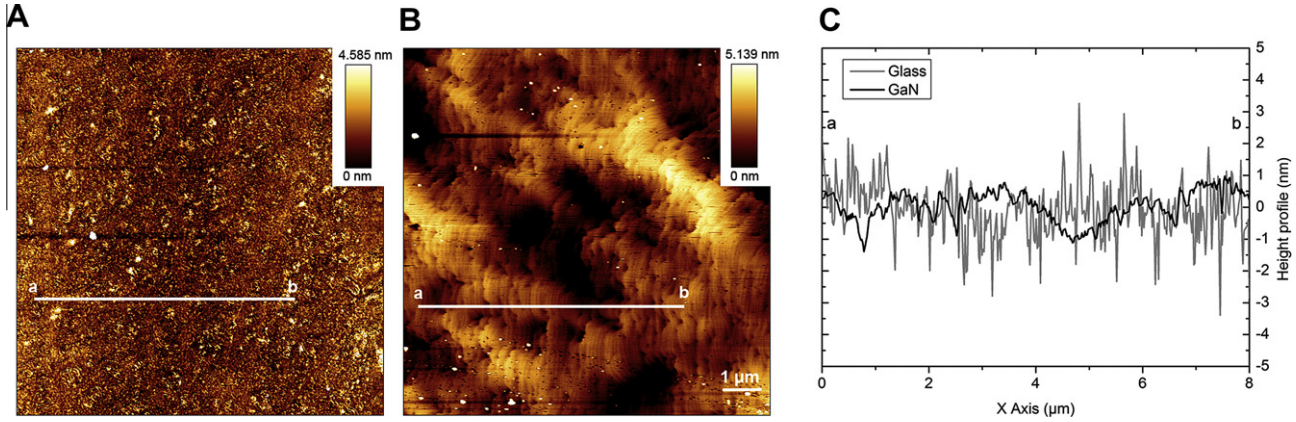

Fig. 2. AFM images of a $10 \times 10\ \mu m^2$ area on (A) a microscope slide glass surface and (B) an n-type GaN surface. The rms surface roughness of glass is 1.0 nm and the rms surface roughness of GaN is 1.2 nm. Despite the similarity of these rms values, the surface morphologies are significantly different. This fact is also observable in the cross sections in (C).

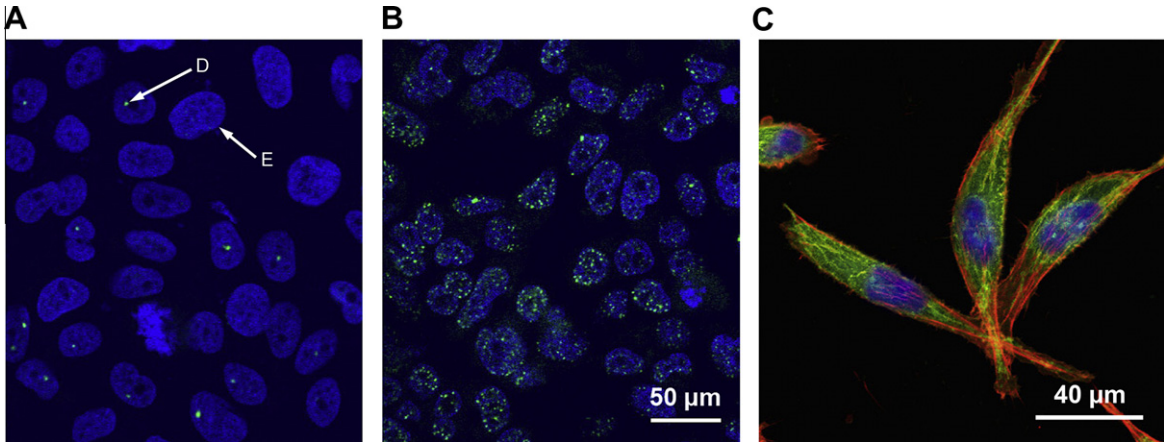

Fig. 3. Stained DNA double strand break repair foci (D, green) and cell nuclei (E, blue) on GaN surfaces for (A) pre- and (B) post-250 mGy air kerma irradiated samples. (C) Three-color staining of fixed cells showing that the cells have excellent morphology. (For interpretation of the references to colour in this figure legend, the reader is referred to the web version of this article.)

difference between the microscope glass slides and GaN was so large that the oxygen-terminated GaN was reproducibly better regarding cell adhesion than the fibronectin-coated glass slides. Static water contact angle measurements revealed a contact angle in the lower percental range for highly hydrophilic glassware compared to ~80° for untreated GaN surfaces. We therefore conclude that structural differences rather than the inherent chemical properties of the two materials were dominant and further comparison of cell growth and proliferation is not presented here.

3.2. Cell repair dynamics on gallium nitride

Cellular DNA repair dynamics from X-ray induced radiation damage were obtained for cells grown on fibronectin coated gallium nitride in order to determine possible material-cell interactions. Alterations in cell repair dynamics would indicate surface-cell interactions. DNA repair dynamics of fibroblasts are well characterized [25] and a comparison of results from the GaN surface to reference measurements made on glass substrates allows conclusions regarding cell functionality. We note that since cells are in direct contact with the GaN capping layer of the HEMT structure, no significant difference is expected between HEMT and homogeneous GaN films. Nevertheless, HEMT hetrostructures were investigated due to their ability to function as biosensors [11–14].

Cells grown on fibronectin-coated GaN surfaces were irradiated with X-rays with different air kerma doses after 24 h of cell growth, and were fixed after certain repair times. Both the DNA repair foci and the cell nuclei were stained and z-stack images were recorded with a laser scanning microscope. Stained DNA double strand break repair foci (green) and cell nuclei (blue) on GaN surfaces for pre- and post-250 mGy air kerma dose irradiated samples are presented in Fig. 3A and B, respectively. A three-color staining of fixed cells on the gallium nitride surface is shown in Fig. 3C. The cell membrane was labeled with DiO (green), F-actin with Rhodamine Phalloidin (red), and cell nuclei with Hoechst 33342 (blue).

Table 1
The average number of foci per single cell as a function of repair time for different air kerma radiation doses. The fitted τ values represent the mean lifetime ($1/e$) from the fits of the exponential decays of the foci counts.

Air kerma dose (mGy)	Foci/cell (Counts) After 30 min	Foci/cell (Counts) After 2 h	Foci/cell (Counts) After 6 h	Foci/cell (Counts) After 24 h	Fitted τ value (d)
0	0.65	0.76	0.94	0.93	
10	2.49	1.56	1.31	1.02	4.06
50	7.14	5.75	2.93	2.66	7.46
100	8.52	6.69	4.48	3.10	9.44
250	16.94	11.93	9.88	5.39	11.73

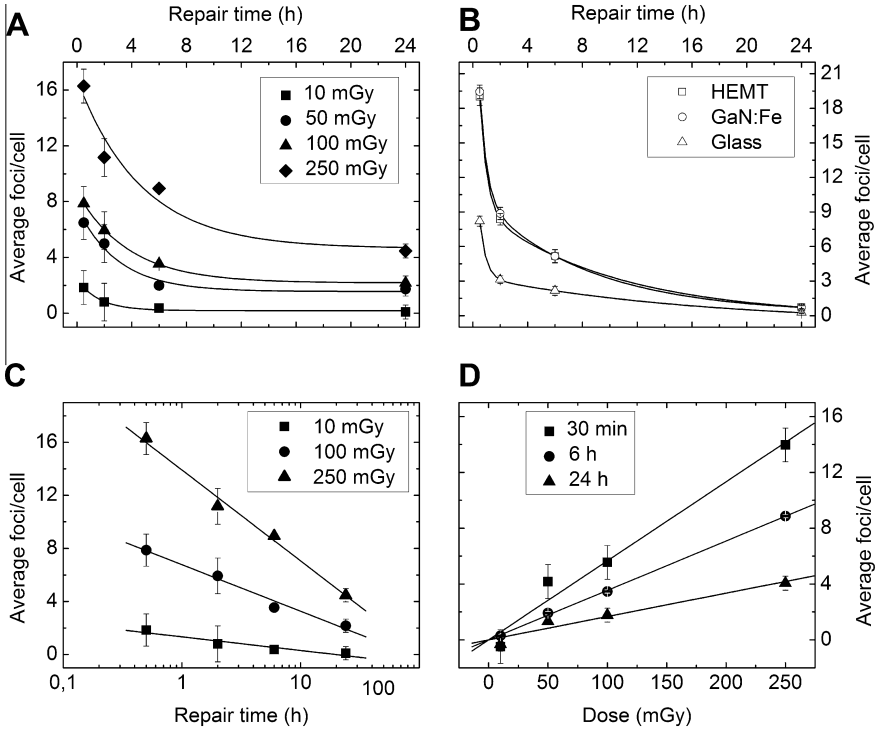

Fig. 4. Repair dynamics of irradiated cells on GaN and glass surfaces. (A) The exponential decay of foci counts as a function of repair time for cells seeded on a fibronectin coated GaN surface is given for different air kerma. (B) Relative repair dynamics of irradiated cells (100 mGy air kerma) on fibronectin coated surfaces in fluid is shown for the different substrates. Although the cells on the GaN surface are exposed to a higher dose due to secondary electrons, the difference in remaining cell damage after 24 h is negligible. (C) A linear-logarithmic plot of the data from (A) shows that these data are characterized by a single exponential decay. (D) The dose–response curve is presented for the data from (A).

The cell shapes and nuclei are clearly observed and show that the cells have excellent morphology. Due to the chemical tolerance and physical stability of the material, it is possible accomplish the staining process directly on the gallium nitride surface. Moreover, the material can also be used as a substrate in confocal laser scanning microscopy as it is transparent in the visible range.

The numerical results of the DNA repair dynamics on GaN surfaces are presented in Table 1 and are plotted in Fig. 4A. Each data point represents the average of counted foci from over 200 evaluated cells. Error bars are calculated from the standard deviation of the linear regression of the dose response curve in Fig. 4D. Since the repair protein 53PB1 requires a certain time to accumulate at the double strand breaks, the initial data points were recorded after a delay time of 30 min had elapsed [27]. For each repair time, a sham irradiated sample, with 0 mGy irradiation, was produced in order to provide a reference for the background foci. In Fig. 4, these background foci were subtracted and only the radiation-induced numbers are given. In comparison to the literature [26], the obtained results show that repair mechanisms are not influenced by the sensor surfaces in any significant way. After 24 h of repair time, 60% of the double strand breaks were repaired, independent of the irradiation dose. This indicates an unrestricted vitality of the cells since an effective DNA repair is preserved. Furthermore, Fig. 4C, which is a linear-logarithmic plot of Fig. 4A, reveals a single exponential decay of the repair foci, thus indicating a complete repair time of approximately 100 h. Fig. 4D shows the dose–response curve of the foci evaluated. Since the total offsets of the curves are due to systematic errors in our dose measurements, the offset is corrected in such a way that the fits of the curves cross the point of origin.

In addition, we compared the repair dynamics between cells cultivated on GaN and glass slides, both of which were coated with fibronectin. The samples were both irradiated and stained simultaneously and every data point represents counted foci from 100 evaluated cells. In contrast to the results in Fig. 4A, the samples were irradiated in fluid, which leads to an increase of absorbed dose due to an additional production of secondary electrons, as can be seen in Fig. 4B. This also has the effect of producing a secondary exponential component in the data, which is true for both the glass and GaN. The error bars represent the standard error of the mean (SEM), since a linear regression of the curve is not applicable. We note that the error bars in Fig. 4B are smaller since the SEM is calculated for each point and the model of the linear dose–response relationship is not considered for the plot. While both samples were exposed to the air kerma of 100 mGy, cells on the GaN surface showed more initial foci than the cells on the glass surface. Sham irradiations showed that this is not a toxic effect from the material. Rather, the semiconductor layer structure advances internal reflection and back-scattering processes. Nevertheless, cells on both GaN and glass samples exhibit similar repair dynamics. After a repair time of 24 h, cells on the GaN sample showed 2.36 foci/cell and cells on the glass substrate 1.66 foci/cell. Considering a background of approximately 0.8 foci/cell, nearly all DNA damage is repaired and there is no significant difference in cell damage. The fitted τ_s value (mean lifetime) of the slow component of the second order exponential decay for cells on the HEMT sample is $\tau_s = 9.74$ d and therefore comparable to the 100 mGy irradiation in Fig. 4A. From these experiments, we found no negative effects of GaN on cell repair dynamics.

In conclusion, we have performed biocompatibility and biofunctionality studies on gallium nitride as a substrate material for various sensor applications. Excellent cell growth behavior was observed on the surfaces, both with and without functional coatings, and stable and reproducible growth dynamics were achieved. Although silanized surfaces created by reaction with aminopropylsilane are known to enhance biocompatibility on similar surfaces

[25] and could provide enhancements for future biosensing applications, surface roughness remains a primary determining factor for biocompatibility at these chain lengths. While DNA repair is one of many mechanisms involved in cell homeostasis, measurement of its dynamics provides a sophisticated method for testing biofunctionality and represents a complementary technique to qualitative analysis and morphological examinations. Here, we did not find any negative effects on cell functionality arising from surface-cell interactions. Furthermore, no significant differences in cell repair dynamics were observed from our comparison of GaN to glass surfaces. This demonstrates that the technique can be used to evaluate cell functionality due to surface–cell interaction effects, which measurements of cell proliferation and growth dynamics are incapable of resolving due to their strong dependence on surface roughness. Our results demonstrate that GaN surfaces have proper biocompatible and biofunctional properties that make devices based on this material an excellent candidate for highly sensitive biofunctional-sensing applications.

Acknowledgments

This work was supported by the German Excellence Initiative via the Nanosystems Initiative Munich (NIM) and the Technische Universität München – Institute for Advanced Study, funded by the German Excellence Initiative. We thank Sabine Konzack, Robin Materlik, and Terry R. Heidmann for experimental work.

References

[1] L. Bousse, Whole cell biosensors, Sensor. Actuat. B-Chem. 34 (1996) 270–275.
[2] J. Yu, S.K. Jha, L. Xiao, Q. Liu, P. Wang, C. Surya, M. Yang, AlGaN/GaN heterostructures for non-invasive cell electrophysiological measurements, Biosens. Bioelectron. 23 (2007) 513–519.
[3] R.G. Richards, The effect of surface roughness on fibroblast adhesion in vitro, Injury 23 (1996) 38–43.
[4] W.M. Reichert, A.A. Sharkawy, Handbook of Biomaterials Evaluation: Scientific, Technical, and Clinical Testing of Implant Materials, vol. 28, Taylor and Francis, Philadelphia, 2000.
[5] C.A. Thomas Jr., P.A. Springer, G.E. Loeb, Y. Berwald-Netter, L.M. Okun, A miniature microelectrode array to monitor the bioelectric activity of cultured cells, Exp. Cell Res. 74 (1972) 61–66.
[6] P. Connolly, P. Clark, A.S.G. Curtis, J.A.T. Dow, C.D.W. Wilkinson, An extracellular microelectrode array for monitoring electrogenic cells in culture, Biosens. Bioelectron. 5 (1990) 223–234.
[7] F. Heer, W. Franks, A. Blau, S. Taschini, C. Ziegler, A. Hierlemann, H. Baltes, CMOS microelectrode array for the monitoring of electrogenic cells, Biosens. Bioelectron. 20 (2004) 358–366.
[8] P. Bergveld, J. Wiersma, H. Meertens, Extracellular potential recordings by means of a field effect transistor without gate metal, called OSFET, IEEE Trans. Biomed. Eng. 23 (1976) 136–144.
[9] M. Hofstetter, J. Howgate, I.D. Sharp, M. Stutzmann, S. Thalhammer, Development and evaluation of gallium nitride-based thin films for X-ray dosimetry, Phys. Med. Biol. 56 (2011) 3215–3231.
[10] G. Steinhoff, M. Hermann, W.J. Schaff, L.F. Eastman, M. Stutzmann, M. Eickhoff, PH response of GaN surfaces and its application for pH-sensitive field-effect transistors, Appl. Phys. Lett. 83 (2003) 177–179.
[11] G. Steinhoff, O. Purrucker, M. Tanaka, M. Stutzmann, M. Eickhoff, $Al_xGa_{1-x}N$-A new material system for biosensors, Adv. Funct. Mater. 13 (2003) 841–846.
[12] G. Steinhoff, B. Baur, G. Wrobel, S. Ingebrandt, A. Offenhäusser, A. Dadgar, A. Krost, M. Stutzmann, M. Eickhoff, Recording of cell action potentials with AlGaN/GaN field-effect transistors, Appl. Phys. Lett. 86 (2005) 033901.
[13] M. Hofstetter, J. Howgate, I.D. Sharp, M. Funk, M. Stutzmann, H.G. Paretzke, S. Thalhammer, Real-time x-ray response of biocompatible solution gate AlGaN/GaN high electron mobility transistor devices, Appl. Phys. Lett. 96 (2010) 092110.
[14] E. Estephan, C. Larroque, F.J.G. Cuisinier, Z. Bálint, C. Gergely, Tailoring GaN semiconductor surfaces with biomolecules, J. Phys. Chem. B 112 (2008) 8799–8805.
[15] I. Cimalla, F. Will, K. Tonisch, M. Niebelschütz, V. Cimalla, V. Lebedev, G. Kittler, M. Himmerlich, S. Krischok, J.A. Schaefer, M. Gebinoga, A. Schober, T. Friedrich, O. Ambacher, AlGaN/GaN biosensor—effect of device processing steps on the surface properties and biocompatibility, Sensor. Actuat. B-Chem. 123 (2007) 740–748.
[16] A.R. Collins, M. Ai-guo, S.J. Duthie, The kinetics of repair of oxidative DNA damage (strand breaks and oxidised pyrimidines) in human cells, Mutat. Res. 336 (1995) 69–77.
[17] Y. Aylon, M. Kupiec, DSB repair: the yeast paradigm, DNA Repair 3 (2004) 797–815.
[18] J.F. Ward, The yield of DNA double-strand breaks produced intracellularly by ionizing radiation: a review, Int. J. Radiat. Biol. 57 (1990) 1141–1150.
[19] S.J. Schoell, M. Hoeb, I.D. Sharp, W. Steins, M. Eickhoff, M. Stutzmann, M.S. Brandt, Functionalization of 6H-SiC surfaces with organosilanes, Appl. Phys. Lett. 92 (2008) 153301.
[20] B. Baur, G. Steinhoff, J. Hernando, O. Purrucker, M. Tanaka, B. Nickel, M. Stutzmann, M. Eickhoff, Chemical functionalization of GaN and AlN surfaces, Appl. Phys. Lett. 87 (2005) 263901.
[21] J. Howgate, S.J. Schoell, M. Hoeb, W. Steins, B. Baur, S. Hertrich, B. Nickel, I.D. Sharp, M. Stutzmann, M. Eickhoff, Photocatalytic cleavage of self-assembled organic monolayers by UV-induced charge transfer from GaN substrates, Adv. Mater. 22 (2010) 2632–2636.
[22] L. Guemouri, J. Ogier, Z. Zekhnini, J.J. Ramsden, The architecture of fibronectin at surfaces, J. Chem. Phys. 113 (2000) 8183–8186.
[23] D. Berdat, A. Marin, F. Herrera, M.A.M. Gijs, DNA biosensor using fluorescence microscopy and impedance spectroscopy, Sensor. Actuat. B-Chem. 118 (2006) 53–59.
[24] F.R. Kloss, M. Najam-Ul-Haq, M. Rainer, R. Gassner, G. Lepperdinger, C.W. Huck, G. Bonn, F. Klauser, X. Liu, N. Memmel, E. Bertel, J.A. Garrido, D. Steinmüller-Nethl, Nanocrystalline diamond—An excellent platform for life science applications, J. Nanosci. Nanotechnol. 7 (2007) 4581–4587.
[25] M. Mahmoodi, L. Ghazanfari, Fundamentals of biomedical applications of biomorphic SiC, in: R. Gerhardt (Eds.), Properties and Applications of Silicon Carbide, InTech, Rijeka, 2011, pp. 297–344.
[26] K. Rothkamm, M. Löbrich, Evidence for a lack of DNA double-strand break repair in human cells exposed to very low X-ray doses, Proc. Natl. Acad. Sci. USA 100 (2003) 5057–5062.
[27] L. Anderson, C. Henderson, Y. Adachi, Phosphorylation and rapid relocalization of 53BP1 to nuclear foci upon DNA damage, Mol. Cell. Biol. 21 (2001) 1719–1729.